

Optical Engineering

SPIDigitalLibrary.org/oe

Improved iterative algorithm for the three-flat test

Bo Gao
Qiang Li
Yuhang He
Liqun Chai

Improved iterative algorithm for the three-flat test

Bo Gao,^a Qiang Li,^a Yuhang He,^a and Liqun Chai^{a,*}

^aFine Optical Engineering Research Center, Ke Yuan Road, Chengdu 610041, China

Abstract. An iterative algorithm has been successfully used to process data from the three-flat test. On the basis of the iterative algorithm proposed by Vannoni, which is much faster and more effective than the Zernike polynomial fitting method, an improved algorithm is presented. By optimizing the iterative steps and removing the scaling factors, the surface shape can be easily computed in a few iterations. The validity of the method is proved by computer simulation, and the interpolation error and principle error are analyzed. © The Authors. Published by SPIE under a Creative Commons Attribution 3.0 Unported License. Distribution or reproduction of this work in whole or in part requires full attribution of the original publication, including its DOI. [DOI: 10.1117/1.OE.53.9.092004]

Keywords: three-flat test; iterative algorithm; computer simulation.

Paper 140007SS received Jan. 2, 2014; revised manuscript received Mar. 12, 2014; accepted for publication Mar. 13, 2014; published online Apr. 16, 2014; corrected Jun. 4, 2014.

1 Introduction

The three-flat test method is generally adopted to measure absolute flatness. Schulz and Schwider proposed and developed the earliest three-flat test method, which required three flats to be compared in pairs.^{1,2} Three measurements could determine only the profile of one diameter. To reconstruct the three-dimensional surface data, many methods have been introduced in which additional measurements are added, e.g., one of the three plates is rotated at least once. Among these methods, the Zernike polynomial fitting method proposed by Fritz is one of the most remarkable.³⁻⁸ To cover more frequencies of the reconstructed surface, more polynomials must be fitted, so the computation is much more intensive. To solve this problem, in recent years Vannoni and Molesini proposed an iterative algorithm⁹⁻¹⁶ to reconstruct the surface shape numerically. The principle of this method is to reconstruct three virtual flats by comparing combinations of their real measurements. Fitting is replaced by rotation or flipping operations, which can be easily and quickly performed.

Vannoni's paper proved the validity of the iterative algorithm. To achieve convergence toward the minimum, thousands of iterations are required. By optimizing the iterative steps and removing scaling factors, the iterative approach we present requires fewer iterations and is less time consuming than Vannoni's method. In this paper, the principle of the new iterative algorithm is introduced, and the validity and advantages of the method are demonstrated by computer simulation. Finally, the interpolation error and principle error are analyzed.

2 Principle

First, an additional rotational measurement is introduced in addition to the traditional three measurements. The Cartesian coordinates and test sequence of the four measurements are shown in Fig. 1.

The four measurements can be expressed as

$$\begin{aligned} W_1 &= K + L, & W_2 &= K + L_R, \\ W_3 &= L_F + M, & W_4 &= K + M. \end{aligned} \quad (1)$$

In Eq. (1), K , L , and M denote the surfaces of the three flats to be measured. L_R denotes the surface data of L after rotation by an angle about the optical axis and L_F represents the flipped data of L about the y -axis. Naturally, the flat after two flips is equal to the unflipped pattern. Further, the flat after rotation back by the same angle is equal to the unrotated pattern.

We denote rotating back by the subscript “-R.” Therefore, if W_2 is rotated back and W_3 is flipped about the y -axis, we can express them as

$$(W_2)_{-R} = K_{-R} + L, \quad (W_3)_F = L + M_F. \quad (2)$$

Thus, according to Eqs. (1) and (2), K , L , and M can be expressed as

$$\begin{aligned} K &= \frac{W_1 + W_2 + W_4}{3} - \frac{M + L_R + L}{3}, \\ L &= \frac{W_1 + (W_2)_{-R} + (W_3)_F}{3} - \frac{K + K_{-R} + M_F}{3}, \\ M &= \frac{W_3 + W_4}{2} - \frac{K + L_F}{2}. \end{aligned} \quad (3)$$

Then, the iterative algorithm is as follows:

1. Initialize the surface data for the three flats (K , L , and M) at zero, which corresponds to starting with the absolute plane.
2. Correct the surface data. The new surface data, K_{new} , L_{new} , and M_{new} , can be calculated as

$$\begin{aligned} K_{\text{new}} &= \frac{W_1 + W_2 + W_4}{3} - \frac{M + L_R + L}{3}, \\ L_{\text{new}} &= \frac{W_1 + (W_2)_{-R} + (W_3)_F}{3} \\ &\quad - \frac{K_{\text{new}} + (K_{\text{new}})_{-R} + M_F}{3}, \\ M_{\text{new}} &= \frac{W_3 + W_4}{2} - \frac{K_{\text{new}} + (L_{\text{new}})_F}{2}. \end{aligned} \quad (4)$$

Equation (4) can be written as

*Address all correspondence to: Liqun Chai, E-mail: chailiqun@163.com

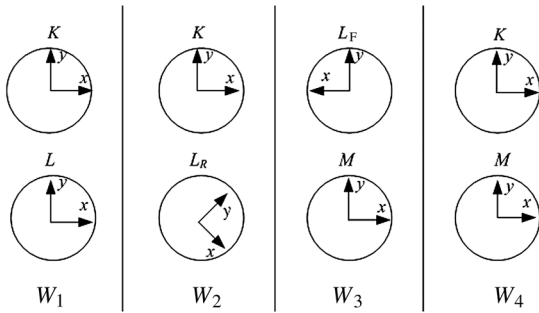


Fig. 1 Four configurations and corresponding measurements.

$$\begin{aligned}
 K_{\text{new}} &= X - \frac{M + L_R + L}{3}, \\
 L_{\text{new}} &= Y - \frac{K_{\text{new}} + (K_{\text{new}})_{-R} + M_F}{3}, \\
 M_{\text{new}} &= Z - \frac{K_{\text{new}} + (L_{\text{new}})_F}{2},
 \end{aligned} \tag{5}$$

where X , Y , and Z are defined as

$$\begin{aligned}
 X &= \frac{W_1 + W_2 + W_4}{3}, \\
 Y &= \frac{W_1 + (W_2)_{-R} + (W_3)_F}{3}, \\
 Z &= \frac{W_3 + W_4}{2},
 \end{aligned} \tag{6}$$

respectively. Because W_1 , W_2 , W_3 , and W_4 do not vary, Eq. (6) can be calculated before the iterative process.

3. Establish the iterative estimation rule. The difference between the reconstructed data and the real measurement data is calculated as follows:

$$\begin{aligned}
 E_1 &= W_1 - K_{\text{new}} - L_{\text{new}}, \\
 E_2 &= W_2 - K_{\text{new}} - (L_{\text{new}})_R, \\
 E_3 &= W_3 - (L_{\text{new}})_F - M_{\text{new}}, \\
 E_4 &= W_4 - K_{\text{new}} - M_{\text{new}}.
 \end{aligned} \tag{7}$$

From Eq. (7), we can obtain

$$\text{EF} = \sqrt{E_1^2 + E_2^2 + E_3^2 + E_4^2}, \tag{8}$$

where EF denotes the reconstruction error. The root-mean-square (rms) value of the EF is calculated and compared with a prespecified threshold. The algorithm should return to step 2 if the threshold is exceeded, and finish otherwise. Figure 2 shows a flow chart of the algorithm.

3 Experiment

To verify the accuracy of the method and compare it with Vannoni's method, three flats were measured, and the data were processed using the proposed iterative algorithm.

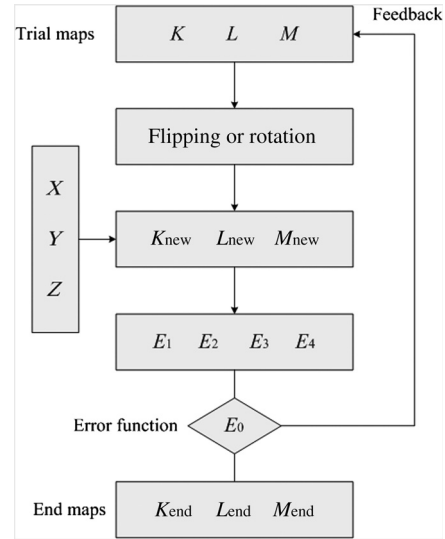


Fig. 2 Schematic flow chart of the iterative algorithm.

In Fig. 3, K , L , and M are the three measured surfaces, which are all circular pupils 920 pixels in diameter.

W_1 , W_2 , W_3 , and W_4 are the four wavefronts processed according to Eq. (1), as shown in Fig. 4. In our case, L is rotated by 54 deg, and L is flipped about the y -axis.

The two methods were tested using the same personal computer with a 3.0 GHz CPU and 2 GB of memory. As Fig. 5 shows the EF of our iterative algorithm approaches the minimum after 10 iterations, whereas Vannoni's approaches the minimum after more than 100 iterations. Apparently our iterative algorithm converges more quickly than that of Vannoni.

In addition, a residual error in L is generated after 128 iterations through subtraction of the actual surface shown in Fig. 5. The rms of the residual error generated by our method is 0.28 nm, whereas that of Vannoni's method is 0.36 nm. Moreover, Vannoni's method leaves many low frequencies, as shown in Fig. 6(a).

4 Error Analysis

The main error sources in this method are the interpolation error and principle error.

4.1 Interpolation Error

The flaw in our method is that the residual error between the reconstructed surface and the measured surface will not decrease after 100 iteration steps, as confirmed by the computer simulation. The main reason is that the error caused by the rotation matrix will accumulate with every iterative loop. In Eq. (2), we assumed that

$$L = (L_R)_{-R}. \tag{9}$$

Actually, the surface data are discrete, so there is an interpolation error due to the rotation operation, which will accumulate.

To eliminate this error, we introduce the term $L - (L_R)_{-R}$ into Eq. (2). Consequently, Eq. (5) in step 2 becomes

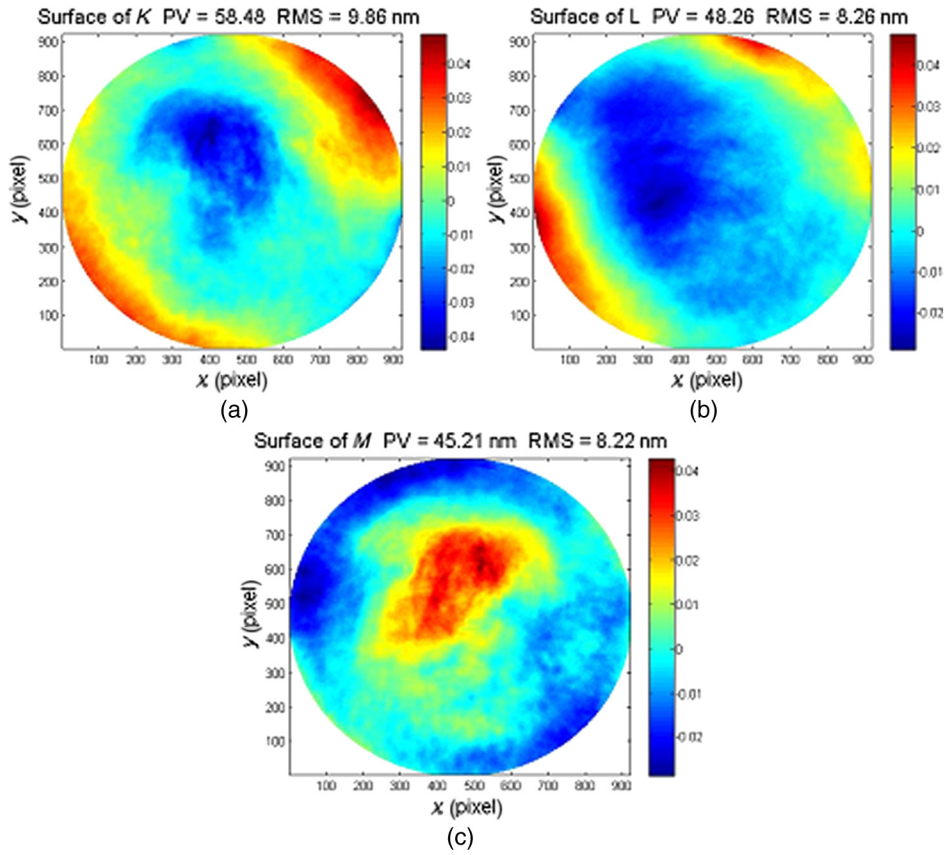


Fig. 3 Surface maps of (a) *K*, (b) *L*, and (c) *M*.

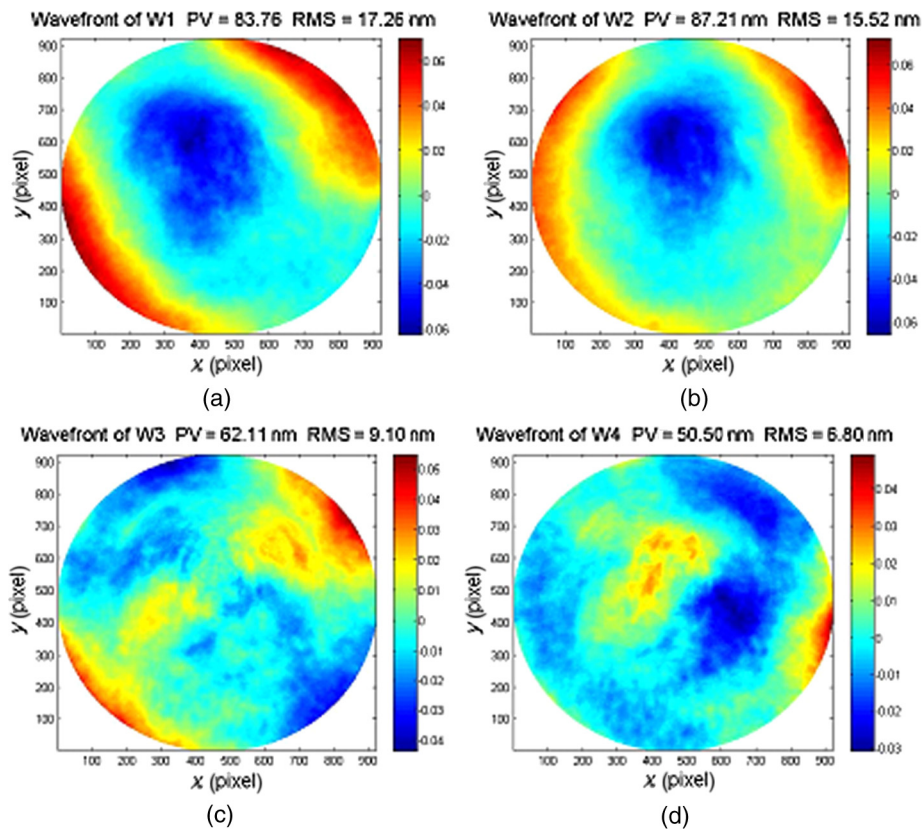


Fig. 4 Wavefronts of (a) *W*₁, (b) *W*₂, (c) *W*₃, and (d) *W*₄.

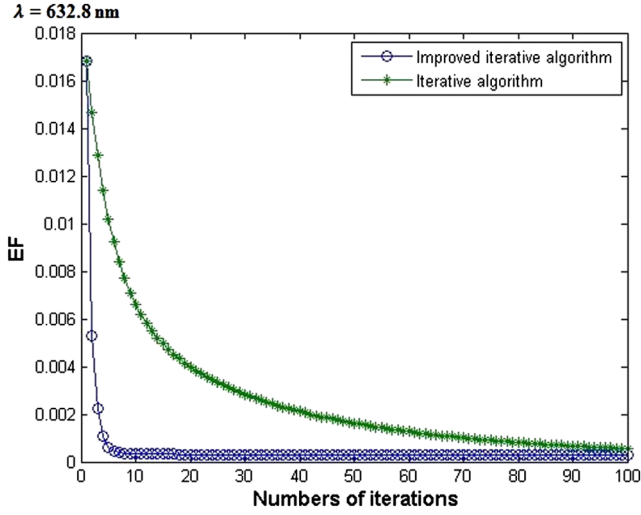


Fig. 5 Error function versus number of iteration cycles.

$$\begin{aligned}
 K_{\text{new}} &= X - \frac{M + L_R + L}{3}, \\
 L_{\text{new}} &= Y - \frac{K_{\text{new}} + (K_{\text{new}})_{-R} + M_F}{3} + \frac{L_{\text{new}}}{3} - \frac{[(L_{\text{new}})_R]_{-R}}{3}, \\
 M_{\text{new}} &= Z - \frac{K_{\text{new}} + (L_{\text{new}})_F}{2}.
 \end{aligned} \tag{10}$$

Figure 7 shows the residual map between the reconstructed surface L and the measured one after 128 iterations. Figures 7(a) and 7(b) are the results of subtraction computed using Eqs. (5) and (10), respectively. The rms of the error shown in Fig. 7(b) is only one-half of that shown in Fig. 7(a). From the image, we can see that the interpolation error is almost eliminated.

4.2 Principle Error

The arbitrary surface can be fitted by a Zernike polynomial. Thus, the surface L is given by

$$L(r, \theta) = \sum_{m,n} U_n^m(r) [L_n^m \cos(m\theta) + L_n^{-m} \sin(m\theta)] \tag{11}$$

and the surface L_F is given by

$$L_F(r, \theta) = \sum_{m,n} U_n^m(r) [\overline{L}_n^m \cos m(\pi - \theta) + \overline{L}_n^{-m} \sin m(\pi - \theta)]. \tag{12}$$

Equation (12) can be expressed as

$$L_F(r, \theta) = \sum_{m,n} U_n^m(r) [L_n^{-m} \sin(m\theta) - L_n^m \cos(m\theta)] \tag{13}$$

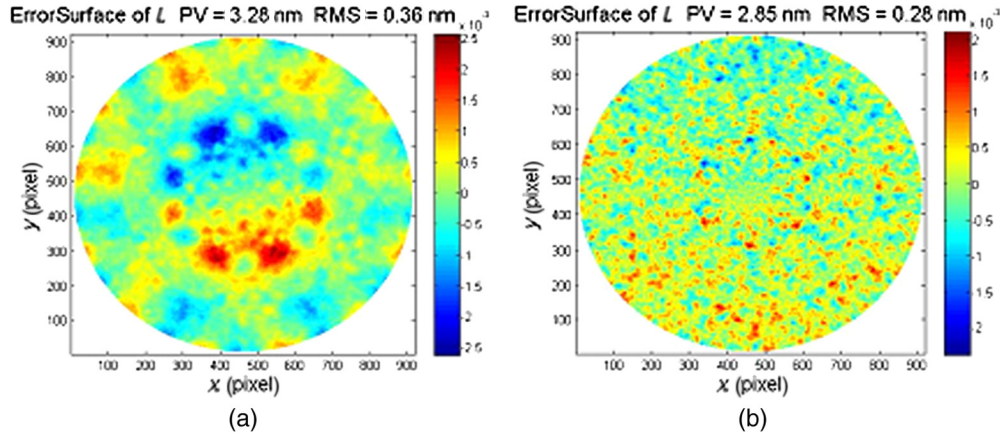


Fig. 6 Residual maps of L after 128 iterations: (a) Vannoni's method and (b) our method.

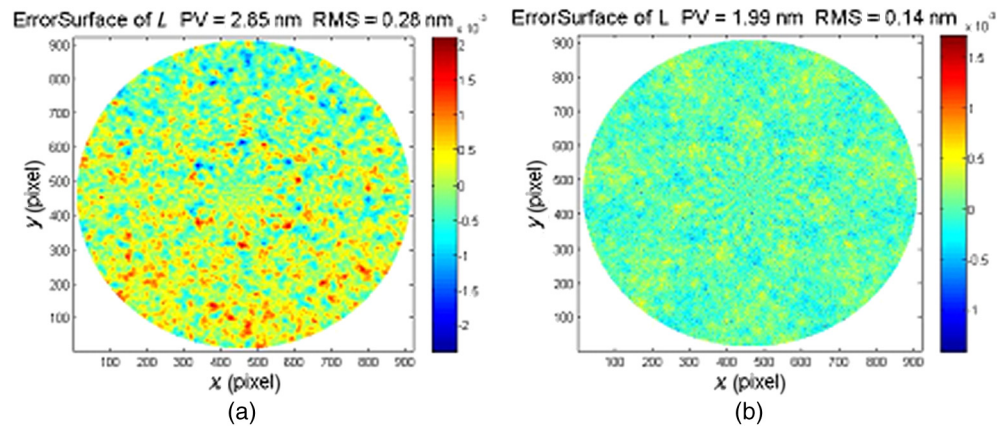


Fig. 7 Residual maps of L after 128 iterations: our method (a) before modification and (b) after modification.

and the surface L_R is

$$L_R(r, \theta) = L(r, \theta - \varphi) \\ = \sum_{m,n} U_n^m(r) [\overline{L}_n^m \cos(m\theta) + \overline{L}_n^{-m} \sin(m\theta)], \quad (14)$$

where

$$\overline{L}_n^m = L_n^m \cos(m\phi) - L_n^{-m} \sin(m\phi), \\ \overline{L}_n^{-m} = L_n^{-m} \cos(m\phi) + L_n^m \sin(m\phi), \quad (15)$$

and φ is the rotation angle. When $m\varphi$ is a multiple of 360 deg, Eq. (15) becomes

$$\overline{L}_n^m = L_n^m, \quad \overline{L}_n^{-m} = L_n^{-m}. \quad (16)$$

Therefore, Eq. (14) is the same as Eq. (11). Further, W_1 is equal to W_2 in Eq. (1). Here, we assume that

$$L(r, \alpha) = L_{\text{even}} + L_{\text{odd}}. \quad (17)$$

Thus,

$$L_F(r, \alpha) = L_{\text{even}} - L_{\text{odd}}, \quad (18)$$

where α is a multiple of 360 deg and φ .

Equation (1) becomes

$$w_1 = K + L_{\text{even}} + L_{\text{odd}}, \\ w_2 = w_1, \\ w_3 = L_{\text{even}} - L_{\text{odd}} + M, \\ w_4 = K + M, \quad (19)$$

where $w_1, w_2, w_3,$ and w_4 include only the part that is a multiple of 360 deg and φ .

According to Eq. (19), L_{even} is

$$L_{\text{even}} = \frac{w_1 + w_3 - w_4}{2}. \quad (20)$$

According to Eqs. (19) and (20), we can obtain

$$K + L_{\text{odd}} = \frac{w_1 - w_3 + w_4}{2}, \\ M - L_{\text{odd}} = \frac{w_3 - w_1 + w_4}{2}, \\ K + M = w_4. \quad (21)$$

Obviously we cannot obtain the exact value of L_{odd} from Eq. (21). Thus, the part that is a multiple of 360 deg and φ in $K, L,$ and M cannot be reconstructed by our iterative algorithm.

5 Comparison of the Two Algorithms

Our approach is generally faster than that of Vannoni. The main reason is that the iterative algorithm computes the updated surfaces directly from the measurements, without a real “adjustment” of a previous surface profile. Every

computation directly influences the next one, so this algorithm is in principle faster than the earlier one. The adjustment factor used in the original algorithm is critical if we want to optimize the algorithm for maximum speed, and the number of iterations will decrease when the adjustment factor is larger. However, the new algorithm (including the rotation adjustment) is still faster, but we can see that the difference between it and Vannoni’s algorithm is reduced.

Note that the improved algorithm is more accurate than the original one only if we stop both of them after 100 iterations. If we allow them to run until the end, they produce identical results.

6 Conclusion

We present an improved iterative algorithm for the three-flat test based on Vannoni’s method. A numerical simulation showed that the process we designed is faster than that of Vannoni. Our method can be applied for absolute flatness measurement, especially when the number of pixels of the interferometer CCD is increased by thousand folds.

References

1. G. Schulz and J. Schwider, “Precise measurement of planeness,” *Appl. Opt.* **6**(6), 1077–1084 (1967).
2. G. Schulz and J. Schwider, “Establishing an optical flatness,” *Appl. Opt.* **10**(4), 929–934 (1971).
3. B. S. Fritz, “Absolute calibration of an optical flat,” *Opt. Eng.* **23**(4), 379–383 (1984).
4. J. Grzanna and G. Schulz, “Absolute testing of flatness standards at square-grid points,” *Opt. Commun.* **77**(2), 107–112 (1990).
5. G. Schulz and J. Grzanna, “Absolute flatness testing by the rotation method with optimal measuring error compensation,” *Appl. Opt.* **31**(19), 3767–3780 (1992).
6. G. Schulz, “Absolute flatness testing by an extended rotation method using two angles of rotation,” *Appl. Opt.* **32**(7), 1055–1059 (1993).
7. V. Greco et al., “Absolute measurement of planarity with Fritz’s method: uncertainty evaluation,” *Appl. Opt.* **38**(10), 2018–2027 (1999).
8. C. Xu, L. Chen, and J. Yin, “Method for absolute flatness measurement of optical surfaces,” *Appl. Opt.* **48**(13), 2536–2540 (2009).
9. M. Vannoni and G. Molesini, “Iterative algorithm for three flat test,” *Opt. Express* **15**(11), 6809–6816 (2007).
10. F. Morin and S. Bouillet, “Absolute interferometric measurement of flatness: application of different methods to test a 600 mm diameter reference flat,” *Proc. SPIE* **6616**, 66164G (2007).
11. M. Vannoni and G. Molesini, “Absolute planarity with three flat test: an iterative approach with Zernike polynomials,” *Opt. Express* **16**(1), 340–354 (2008).
12. M. Vannoni and G. Molesini, “Three-flat test with plates in horizontal posture,” *Appl. Opt.* **47**(12), 2133–2145 (2008).
13. C. Morin and S. Bouillet, “Absolute calibration of three reference flats based on an iterative algorithm: study and implementation,” *Proc. SPIE* **8169**, 816915 (2011).
14. M. Vannoni and G. Molesini, “Absolute planarity test with multiple measurements and iterative data reduction algorithm,” presented at *SPIE-Optifab*, Rochester, Poster TD06–62 (May 11–14 2009).
15. M. Vannoni, A. Sordini, and G. Molesini, “Calibration of absolute planarity flats: generalized iterative approach,” *Opt. Eng.* **51**(8), 081510 (2012).
16. M. Vannoni, “Absolute flatness measurement using oblique incidence setup and an iterative algorithm: a demonstration on synthetic data,” *Opt. Express* **22**(3), 3538–3546 (2014).

Bo Gao is an assistant professor at the Fine Optical Engineering Research Center. He received his BS and MS degrees in optical engineering from Nanjing University of Science and Technology in 2006 and 2008, respectively. His research focuses on optical manufacturing and testing.

Biographies of the other authors are not available.